The Ekman layer model revisited

Yosef Ashkenazy,[1] Hezi Gildor,[2] and Golan Bel[1]

[1]*Department of Solar Energy and Environmental Physics,*
Blaustein Institutes for Desert Research,
Ben-Gurion University of the Negev, Sede Boqer Campus 84990, Israel

[2]*The Fredy and Nadine Herrmann Institute of Earth Sciences,*
The Hebrew University of Jerusalem, Jerusalem, Israel

(Dated: February 18, 2015)

Abstract

The seminal model for the effect of winds on surface ocean currents was proposed by Ekman more than a century ago. It demonstrated the non-trivial effect of Earth's rotation on surface ocean currents driven by constant wind. Here we show that this model is ill-defined when forced by a more realistic stochastic wind—the component of the stochastic wind that resonates with the Coriolis frequency leads to the divergence of the surface and depth-integrated currents. The addition of a linear friction term to the model suppresses this unphysical divergence. We present explicit solutions for the surface and depth-integrated currents for wind stress with exponentially decaying and oscillating temporal correlations and show that the wind's temporal correlations and the friction drastically affect, and can even diminish, the resonance. Winds and currents from the Gulf of Elat are compared with the model's predictions.

Motivated by the observation of Fridtjof Nansen that ice in the Arctic drifts 20°-40° to the right of the prevailing winds, Vagn Walfrid Ekman [1] developed, in 1905, a simple model for the depth dependence of the surface current under the action of constant (or pulse-like) wind. This highly idealized model predicted a clockwise spiral rotation as a function of depth, an exponentially decaying current speed with depth, an angle of 45° of the surface current to the right of the wind, and integrated currents that are (right) perpendicular to the wind [2–4]. Ekman's model was supported by observations [e.g., 5–8] and by rotating tank experiments [e.g., 3, 9, 10]. The Ekman model is one of the most fundamental models to demonstrate the effect of Earth's rotation on the ocean currents, and basic oceanic processes (like coastal upwelling/ downwelling and Ekman transport) are based on it. However, the simplicity of the Ekman model and its simplistic assumptions (such as the constant eddy parameterized vertical viscosity coefficient) limit its applicability [1] to the atmosphere and ocean.

Many studies have generalized and modified the Ekman model. Yet, only a limited number of studies have investigated the effects of stochastic wind on the surface currents [e.g., 11–15], especially when the wind is temporally correlated [16]. This is especially surprising since winds are stochastic in their nature and are far from being temporally constant as was assumed by Ekman [e.g., 17–19].

Here we study the Ekman layer model under the action of stochastic and temporally correlated wind stress. We demonstrate that the depth-dependent Ekman layer model is ill-defined when forced by stochastic wind stress due to the resonance of the Coriolis force (frequency) with a wind-stress component of corresponding frequency–this resonance eventually leads to the divergence of the surface currents. To avoid this divergence, we follow [20] and add a linear friction term to the Ekman layer model. We present an explicit solution for the surface and depth-integrated currents. We show that the effect of the resonance strongly depends on the temporal correlations of the wind and the friction term.

Based on [1], we study the effect of wind stress on surface ocean currents using the following set of equations

$$u_t - fv = \nu u_{zz} - ru, \tag{1}$$

$$v_t + fu = \nu v_{zz} - rv, \tag{2}$$

where t and z are the time and depth coordinates, u and v are the zonal (west to east)

and meridional (south to north) velocities, f is the Coriolis parameter assumed here to be constant, ν is the eddy parameterized vertical viscosity coefficient, and r is a constant resembling Rayleigh-like friction [20]. Note that the addition of the r terms is crucial for the results of this paper; they are not part of the original Ekman layer model but are added here to solve the problem of the divergence of surface currents under resonance conditions; see below.

By defining a new complex variable $w = u + iv$, it is possible to obtain a single equation for Eqs. (1), (2):

$$w_t + (r + if)w = \nu w_{zz}. \tag{3}$$

After applying a Fourier Transform (FT) with respect to the time variable [33], we obtain the following z-dependent equation:

$$\hat{w}_{zz} - \frac{r + i(f + \omega)}{\nu}\hat{w} = 0. \tag{4}$$

We assume that the ocean is infinitely deep, that the currents vanish at depth, and that at the surface [2]

$$\hat{w}_z(z = 0) = \frac{1}{\rho_0 \nu}(\hat{\tau}_x + i\hat{\tau}_y) = \frac{1}{\rho_0 \nu}\hat{\tau}, \tag{5}$$

where ρ_0 is the water density (assumed here to be constant), and $\hat{\tau}_x$, $\hat{\tau}_y$ are the FT of the zonal and meridional wind-stress components. Under these assumptions and boundary conditions:

$$\hat{w} = \frac{\hat{\tau}}{\rho_0 \nu k} e^{kz}, \tag{6}$$

where

$$k = \frac{(r^2 + (f + \omega)^2)^{1/4}}{\sqrt{\nu}} e^{i\phi/2}; \tag{7}$$

$$\phi = \tan^{-1}\left(\frac{f + \omega}{r}\right), \tag{8}$$

such that

$$|\hat{w}|^2 = \frac{|\hat{\tau}|^2}{\rho_0^2 \nu \sqrt{r^2 + (f + \omega)^2}} e^{2(r^2 + (f+\omega)^2)^{1/4} z/\sqrt{\nu}}. \tag{9}$$

At the surface ($z = 0$), Eq. (9) becomes:

$$|\hat{w}|^2 = \frac{|\hat{\tau}|^2}{\rho_0^2 \nu \sqrt{r^2 + (f + \omega)^2}}. \tag{10}$$

For the integrated currents (Ekman transport) $\hat{W} = \int \hat{w} dz$, we get

$$|\hat{W}|^2 = \frac{|\hat{\tau}|^2}{\rho_0^2 (r^2 + (f + \omega)^2)}. \tag{11}$$

The second moment of the currents, $\langle|w|^2\rangle$, can be obtained by using the Parseval's theorem:

$$\langle|w|^2\rangle = \frac{1}{2\pi}\int_{-\infty}^{\infty}|\hat{w}|^2 d\omega. \tag{12}$$

Thus, once the power spectrum of the wind stress, $|\hat{\tau}|^2$, is known, it is possible to obtain the second moment of the currents.

Consider the case in which the wind stress has exponentially decaying temporal correlations superimposed on a periodic signal (representing, e.g., the diurnal cycle):

$$\langle\tau_x(\tilde{t})\tau_x(\tilde{t}+t)\rangle = \frac{\tau_{0,x}^2}{2}e^{-\gamma_x|t|}\cos(\omega_0 t), \tag{13}$$

where $\tau_{0,x}^2$ is a constant representing the second moment of the wind-stress in the x (zonal) direction, γ_x is the exponential decay rate of the temporal correlations, and ω_0 is the frequency at which the correlation function oscillates [34]. Here, we assume that the zonal and meridional components of the wind-stress are independent such that each component can be analyzed separately and the linearity of the model implies that the overall result is the sum of their contributions. We thus restrict ourselves below to the zonal direction where the generalization to include the meridional direction is straightforward. For simplicity, we drop below the subscript "x".

The FT of Eq. (13) is

$$|\hat{\tau}|^2 = \frac{\gamma\tau_0^2}{2}\left(\frac{1}{\gamma^2+(\omega+\omega_0)^2}+\frac{1}{\gamma^2+(\omega-\omega_0)^2}\right). \tag{14}$$

Hence, in principle, it possible to find the second moment of the depth-dependent currents using Eqs. (9) and (12). However, it seems that there is no general analytic solution for this integral unless the wind stress is periodic and $|\hat{\tau}|^2$ is a delta function. Yet, we find the second moment of the depth-integrated current given in Eq. (11)

$$\langle|W|^2\rangle = \frac{\tau_0^2}{4\rho_0^2}\frac{\gamma+r}{r}\left(\frac{1}{(f+\omega_0)^2+(\gamma+r)^2}+\frac{1}{(f-\omega_0)^2+(\gamma+r)^2}\right). \tag{15}$$

In the absence of periodic wind stress (i.e., $\omega_0 = 0$), this expression is consistent with our previous derivations [16].

It is also possible to obtain an analytic expression for the second moment of the surface currents ($z = 0$) given in Eq. (10):

$$\langle|w|^2\rangle = \frac{\sqrt{2}}{8\pi}\frac{\tau_0^2}{\nu\rho_0^2}\sum_{j=+,-}\frac{1}{B_j}\left[(\pi-2\alpha_j)\sqrt{B_j+A_j}+\sqrt{B_j-A_j}\ln C_j\right], \tag{16}$$

where

$$A_{\pm} = r^2 - \gamma^2 + (f \pm \omega_0)^2 \tag{17}$$

$$B_{\pm} = \sqrt{A_{\pm}^2 + 4\gamma^2 (f \pm \omega_0)^2} \tag{18}$$

$$C_{\pm} = \frac{1}{r^2}\left[(f \pm \omega_0)^2 + B_{\pm} + \sqrt{2}\,|f \pm \omega_0|\,\sqrt{B_{\pm} + A_{\pm}} + \gamma^2 + \sqrt{2}\gamma\sqrt{B_{\pm} - A_{\pm}}\right] \tag{19}$$

$$\tan\alpha_{\pm} = \frac{\sqrt{2}\gamma + \sqrt{B_{\pm} - A_{\pm}}}{\sqrt{2}\,|f \pm \omega_0| + \sqrt{B_{\pm} + A_{\pm}}}. \tag{20}$$

Note that $B_{\pm} \geq |A_{\pm}|$ such that the square roots in Eqs. (19) and (20) are always non-negative.

We will consider below a few limiting cases of the general expression of the second moment of surface currents given in Eqs. (16)-(20).

Constant wind and no friction: In this case, $r = 0$, $\gamma = 0$, and $\omega_0 = 0$. Then the second moment is $\langle |w|^2 \rangle = \tau_0^2/(2\nu\rho_0^2|f|)$. This expression is consistent with the classical solution of Ekman [2, 3, 9].

Infinite friction: In this case, $r \to \infty$ and then $\langle |w|^2 \rangle \to \tau_0^2/(2\rho_0^2\nu r) \to 0$, as expected from the very large friction.

Zero friction: In this case, $r \to 0$ and

$$\langle |w|^2 \rangle \approx -\frac{\gamma \ln r}{2\pi}\frac{\tau_0^2}{\nu\rho_0^2}\left(\frac{1}{\gamma^2 + (f+\omega_0)^2} + \frac{1}{\gamma^2 + (f-\omega_0)^2}\right). \tag{21}$$

Thus the second moment diverges when $r \to 0$, assuming that all other parameters are finite, highlighting the problem with the traditional formulation of the Ekman layer model.

Periodic wind: In this case, $\gamma \to 0$, and when assuming a finite friction r we get

$$\langle |w|^2 \rangle = \frac{\tau_0^2}{4\nu\rho_0^2}\left(\frac{1}{\sqrt{r^2 + (f+\omega_0)^2}} + \frac{1}{\sqrt{r^2 + (f-\omega_0)^2}}\right). \tag{22}$$

When $|f| = |\omega_0|$, the leading order term of $\langle |w|^2 \rangle$ varies like $1/r$ and diverges when $r \to 0$. Intuitively, the latter case is equivalent to a forced harmonic oscillator without friction and under resonance conditions.

Uncorrelated wind: In this case, $\gamma \to \infty$, and when $r > 0$, we get $\langle |w|^2 \rangle = [\tau_0^2/(\pi\nu\rho_0^2)](\ln\gamma)/\gamma \to 0$. Thus, as expected, surface currents are not developed under the action of uncorrelated wind [see also 16].

We summarize the model's results in Fig. 1. In Fig. 1a, we present the mean surface current (in cm/s) as a function of the Coriolis and correlation parameters (f and γ, respectively). The dashed and solid lines indicate the maximal magnitude of the current along the

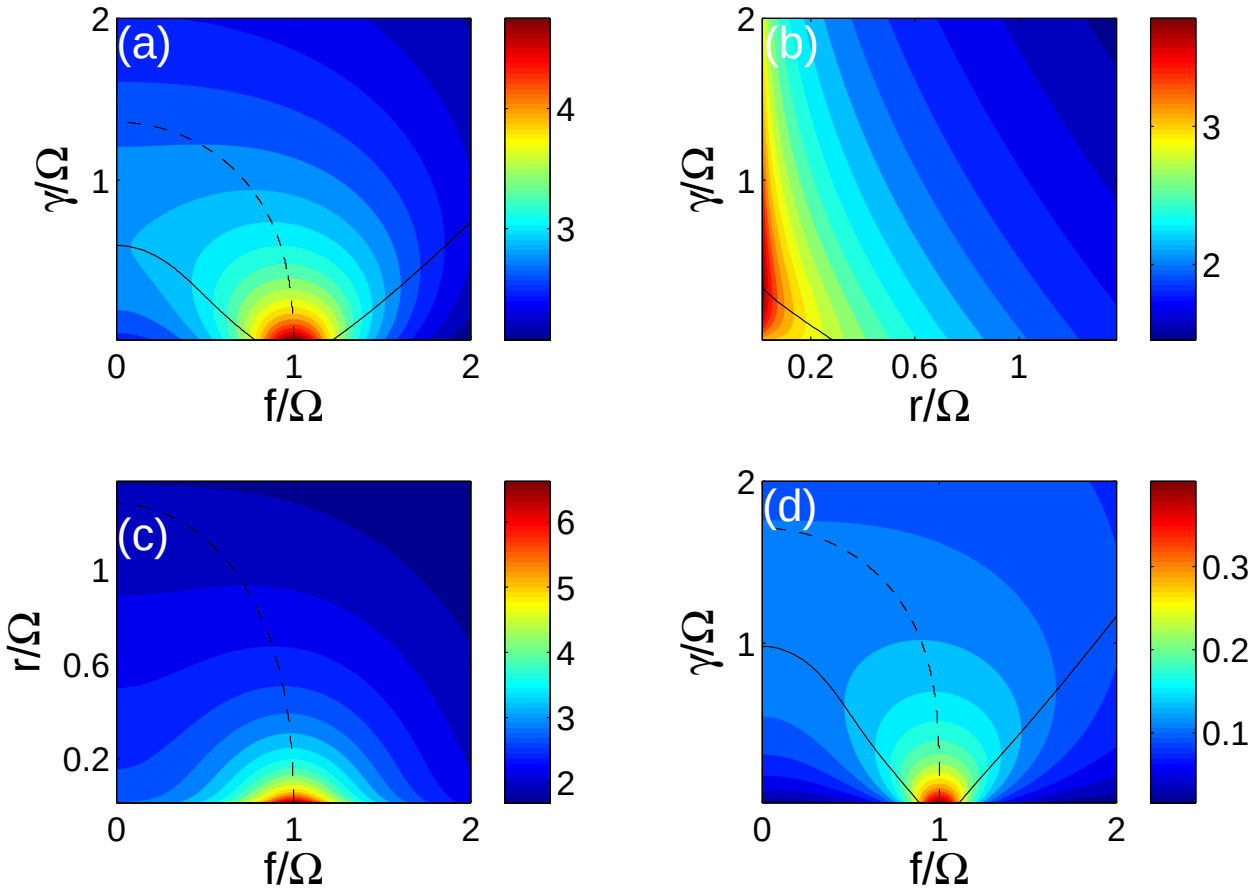

FIG. 1: (a) Mean surface current speed (in cm/s) as a function of the Coriolis parameter (frequency), f, and the temporal correlation parameter, γ. (b) Same as (a) but for the friction parameter r and temporal correlation parameter γ. (c) Same as (a) but for the friction parameter r and the Coriolis parameter f. (d) Same as (a) but for the current at a depth of 400 m. In all panels, the solid line indicates the maximum value along the vertical axis while the dashed line indicates the maximum value along the horizontal axis. Parameter values are: $\Omega = 2\pi/86400$ s^{-1}, $f = 2\Omega\sin(45^\circ)$, $\omega_0 = \Omega$, $\tau_0 = 0.1$ N m^{-2}, $\nu = 0.1$ m^2 s^{-1}, $\rho_0 = 1028$ kg m^{-3}, $r = 10^{-5}$ s^{-1}, $\gamma = 10^{-5}$ s^{-1}.

x (f) and y (γ) axes. For small γ, the maximum (resonance) occurs close to the frequency of the wind (as $\omega_0 = \Omega$), and the current is large there. However, when γ becomes larger, the maximum value occurs at a smaller value of the Coriolis parameter and the maximal current is smaller; for $\gamma/\Omega \geq 1.36$, the maximum disappears and the current speed decreases monotonically as a function of the Coriolis parameter, f. There is also a maximal value as a function of the temporal correlations parameter, γ. A similar optimum was reported in [16]

for the integrated currents. There is no maximum when the Coriolis parameter is close to the frequency of the wind ($f \approx \omega_0$), as the wind resonance with the Coriolis force overcomes the optimum due to the temporal correlations.

Fig. 1b depicts the mean surface current speed as a function of the friction parameter, r, and the temporal correlation parameter, γ. As expected, also here there is an optimum with respect to γ but not with respect to the friction parameter, r. The mean surface current speed as a function of f and r is shown in Fig. 1c where here, as expected, there is an optimum (resonance) with respect to the Coriolis parameter. Yet, similar to Fig. 1a, the optimum occurs for smaller values of the Coriolis parameter as the friction, r, grows; above $r \approx 1.2$, there is no optimum and the surface current speed decreases monotonically with f. Fig. 1d is similar to Fig. 1a except that here, we present the mean current speed at a depth of 400 m. The two are qualitatively similar except that in depth the currents are weaker and there is a wider range for optimal values, i.e., there is an optimal Coriolis parameter for which the z=-400 m current is maximal for $\gamma/\Omega \leq 1.7$, while for the surface current, there is an optimal value for $\gamma/\Omega \leq 1.36$. Interestingly, even at such great depths, much below the surface Ekman layer depth $\sqrt{2\nu/\Omega} \approx 50$ m, there are noticeable currents. This is especially evident for $\gamma \ll 1$ and $f/\Omega \approx 1$ where the resonance is pronounced and the Ekman layer becomes very deep as $f + \omega = 0$ [Eq. (9)]. We obtained similar results to those shown in Fig. 1 when using the depth-integrated currents, using Eq. (15); the underlying mechanism of the optimum with respect to the temporal correlation parameter, γ, was discussed in length in [16], and we conjecture that a similar mechanism stands behind the results presented above.

We examine the predictions of the Ekman layer model described above against current measurements from the Gulf of (Aqaba) Elat, Israel. The results are presented in the supplementary material. The location of the point of measurement is 34.92°E, 29.5°N at which the Coriolis frequency is very close to the diurnal frequency of the wind. Thus, in this location, the wind may resonate with the Coriolis force. Currents were recorded at depths of 10 m, 24 m, 36 m, and 330 m [21, 22]. We compare the monthly mean wind speed to the monthly mean current speed, focusing on two months, January and April 2009. The mean wind speed during April is stronger than that of January (Fig. S1a); yet, the mean current speed during January is much larger than during April (Fig. S1b,d). The resonance of the wind-forced currents with the Coriolis frequency may resolve this apparent contradiction

as the winds have larger power at the diurnal band compared to the background during January 2009 (Fig. S1c).

To examine the effect of the resonance and to estimate the value of the friction coefficient, r, we have integrated Eqs. (1) and (2) using the measured winds in the Gulf of Elat; several Coriolis parameters corresponding to latitudes 20°N, 30°N, and 40°N were considered. January and April 2009 currents at different depths versus r are depicted in Fig. S2. First, it is clear that the simulated currents at 30°N are much stronger than the currents of 20°N and 40°N. Second, we estimate an upper bound for r as the crossing point of r at which the simulated mean January 2009 current becomes smaller than that of April 2009, since the observed currents are stronger than the April 2009 currents. The friction parameter corresponding to the crossing point is larger for deeper currents. Since the observations indicate that the currents during January 2009 are larger than those of April 2009, also at a depth of 10 m, and since the simulated January currents are larger than those of April only when $r < 10^{-6}$ s^{-1} (Fig. S2a), we conclude that $r < 10^{-6}$ s^{-1} for the Gulf of Elat. Alternatively, it is possible that r is depth-dependent.

There are several energy sources for the kinetic energy of the Gulf of Elat, including winds, tides, currents through the Straits of Tiran (the straits that connect the Red Sea with the Gulf of Elat), deep water formation, and geothermal heating [23–26]. Yet, it is apparent that the winds underlie a significant part of the surface currents' kinetic energy. While the example of January versus April 2009 currents provide evidence for the effect of the resonance of the Coriolis force with the wind's frequency, there are counterexamples for which the wind is strong and periodic, and yet the currents are less pronounced (e.g., June 2009, Fig. S1); in such cases, some of the other factors mentioned above may dominate the currents.

The seminal Ekman layer model has been used for more than a century to study the effect of winds on surface currents. Here we show that the surface currents predicted by the Ekman layer model diverge when the wind is stochastic, such that one of its components resonates with the Coriolis frequency. Many studies reported the signature of "inertial" resonance, i.e., enhanced currents as a result of resonance between the Coriolis parameter and the periodicity of the winds [e.g., 12, 27–31] (tides can also resonate with the Coriolis frequency [e.g., 32]). However, the temporal correlations of the wind were largely ignored in the framework of the Ekman layer model. The temporal correlations of the wind play

a significant role in the surface currents–there is an optimal correlation time for which the surface currents' magnitude is maximal [16]. Here, we used the depth-dependent Ekman layer model to show that the temporal correlations of the winds drastically affect the currents (including the resonance of the Coriolis force with the winds) and that without a friction term added to the model, the currents diverge.

Although there are observations that support the predictions of the Ekman layer model [e.g., 6, 7, 29], there is still a large gap between the observations and the model [e.g., 3]. This gap may be attributed to the simplicity of the model, to the constant vertical eddy parameterized viscosity coefficient, to lateral effects, etc. It is possible that the stochastic nature of the wind stress, its temporal correlations and the friction term studied here may help to better fit observations with the predictions of the Ekman layer model.

We thank Georgy Burde and Eli Tziperman for helpful discussions.

[1] V. W. Ekman, Arch. Math. Astron. Phys. **2**, 1 (1905).

[2] A. E. Gill, *Atmosphere–ocean dynamics* (Academic Press, London, 1982) p. 662.

[3] B. Cushman-Roisin, *Introduction to geophysical fluid dynamics*, 1st ed. (Prentice Hall, 1994).

[4] H. Gildor, Geophysical and Astrophysical Fluid Dynamics **102**, 593599 (2008).

[5] K. Hunkins, Deep Sea Res. **13**, 607 (1966).

[6] J. F. Price, R. A. Weller, and R. R. Schudlich, Science **238**, 1534 (1987).

[7] T. K. Chereskin, J. Geophys. Res. **100**, 18261 (1995).

[8] C. J. Roach, H. E. Phillips, N. L. Bindoff, and S. R. Rintoul, Proceedings of the 18th Australasian Fluid Mechanics Conference (2012).

[9] G. K. Vallis, *Atmospheric and Oceanic Fluid Dynamics* (Cambridge University Press, Cambridge, U.K., 2006) p. 745.

[10] J. Marshall and R. A. Plumb, *Atmosphere, Ocean, and Climate Dynamics: An introductory text* (Elsevier Academic Press, 2008).

[11] J. Gonella, Deep Sea Res. **18**, 775 (1971).

[12] J. C. McWilliams and E. Huckle, J. Phys. Oceanogr. **36**, 1646 (2005).

[13] P. C. Chu, IEEE J. of Selected Topics in Applied Earth Observations and Remote Sensing **2**, 27 (2009).

[14] P. C. Chu, Geophys. Res. Lett. **35**, L12606 (2008).

[15] Y. Ashkenazy and H. Gildor, J. Phys. Oceanogr. **41**, 2295 (2011).

[16] G. Bel and Y. Ashkenazy, New J. Phys. **15**, 053024 (2013).

[17] J. V. Seguro and T. W. Lambert, J. Wind Engineering and Industrial Aerodynamics **85**, 75 (2000).

[18] A. H. Monahan, J. Climate **19**, 497 (2006).

[19] A. H. Monahan, J. Climate **23**, 5151 (2010).

[20] S. Y. Kim, P. M. Kosro, and A. L. Kurapov, J. Geophys. Res. **119**, 6631 (2014).

[21] D. F. Carlson, E. Fredj, H. Gildor, E. Biton, J. V. Steinbuck, S. G. Monismith, and A. Genin, J. Mar. Sys. **102**, 14 (2012).

[22] D. F. Carlson, E. Fredj, and H. Gildor, Deep Sea Res. **84**, 1 (2014).

[23] E. Biton, J. Silverman, and H. Gildor, Geophys. Res. Lett. **35**, L14603 (2008).

[24] E. Biton and H. Gildor, J. Geophys. Res. **116**, C08020 (2011).

[25] E. Biton and H. Gildor, J. Geophys. Res. **116**, C08022 (2011).

[26] E. Biton and H. Gildor, J. Phys. Oceanogr. **44**, 1954 (2014).

[27] D. L. Rudnick and A. Weller, R., J. Phys. Oceanogr. **23**, 2359 (1993).

[28] G. B. Crawford and W. G. Large, J. Phys. Oceanogr. **26**, 873891 (1996).

[29] D. L. Rudnick, in *Near-Boundary Processes and Their Parameterization, Proceedings of the 13th 'Aha Huliko'a Hawaiian Winter Workshop*, edited by P. Müller and D. Henderson (University of Hawaii, 2003) pp. 163–170.

[30] J. B. Mickett, Y. L. Serra, M. F. Cronin, and M. H. Alford, J. Phys. Oceanogr. **40**, 401 (2010).

[31] D. B. Whitt and L. N. Thomas, J. Phys. Oceanogr. **45**, 181208 (2015).

[32] R. G. Stockwell, W. G. Large, and R. F. Milliff, Tellus A **56**, 536547 (2004).

[33] The Fourier transform is defined here as $\hat{w}(\omega) \equiv \int_{-\infty}^{\infty} w(t)\, e^{-i\omega t} dt$

[34] When $\tau_x = \tau_{0,x}\cos(\omega_0 t) + \tau_{1,x}\eta_t$ where η_t is a random variable with exponentially decaying correlations and zero mean, then $\langle \tau_x(\tilde{t})\tau_x(\tilde{t}+t)\rangle \approx \tau_{0,x}^2\cos(\omega_0 t)/2 + \tau_{1,x}^2\langle \eta_{t+\tilde{t}}\eta_{\tilde{t}}\rangle/2 = \tau_{0,x}^2\cos(\omega_0 t)/2 + \tau_{1,x}^2 e^{-\gamma_x|t|}/2$. This is the sum of Eq. (13) with $\gamma_x = 0$ plus Eq. (13) with $\omega_0 = 0$.

Supplemental Materials: The Ekman layer model revisited

Below we describe measurements and simulations of the currents in the Gulf of Elat, Israel.

The Gulf of Elat. The Gulf of Elat is a deep (down to ∼2 km), narrow (∼20 km), and long (∼200 km) gulf that is connected to the Red Sea through the Straits of Tiran. The currents in the gulf are mainly driven by the winds and tides. The stratification in the gulf is weak where the salinity is almost constant with time and depth (∼42 grams of salt per kg of water), and the seasonal variations in temperature ranges between ∼27°C in the summer to ∼21°C during winter. The mixed layer depth varies between ∼100 m during summer to almost the entire water column during winter. Water exchange through the Straits of Tiran plays an important role in the circulation of the gulf. The winds in the gulf are mostly northerly.

Measurements. The measurements were taken at the northern tip of the gulf. The shallow depth currents were recorded using a 600 kHz Acoustic Doppler Current Profiler (ADCP) from September 10, 2008 to July 13, 2009 at 29.4882°N 34.926°E (where the water depth is 400 m); the sampling interval was one hour. The deep currents (330 m) were recorded using an S4 electromagnetic current meter from October 12, 2008 to July 12, 2009 at 29.498°N 34.936°E (where the water depth is 400 m), very close to the location of the ADCP; the sampling interval was 20 minutes. For more details, see [S21, S22]. Ten-minute-mean 10-m-height winds were measured at a nearby coastal deck (29.501084°N, 34.916421°E).

Results. The monthly mean and standard deviation of the wind speed are depicted in Fig. S1a–it is clear that the wind was stronger and more variable during April 2009 compared with January 2009. However, the monthly mean shallow depth currents (Fig. S1b) and deep currents (Fig. S1d) were much stronger in January than in April, in spite of the weaker winds during January. We attribute this enhancement of currents to the resonance of the Coriolis frequency, which is very close to the diurnal frequency at latitude 29.5°N of the Gulf of Elat. This hypothesis is supported by Fig. S1c in which we plot the Fourier transform amplitude of the wind speed at the diurnal frequency. We first normalized the wind speed's monthly time series by subtracting the mean and dividing by the standard deviation, to allow a comparison of the diurnal peak of the different months compared with the "noisy" background of the Fourier transform. Clearly, the January wind was more diurnally periodic

than the April wind, making it more favorable to resonate with the Coriolis frequency.

To more deeply understand the effect of the resonance with the Coriolis frequency and the effect of the friction parameter, r, on the dynamics, we numerically solved Eqs. (1) and (2), using the measured winds of Elat described above. In Fig. S2, we plot the mean current speed of January and April 2009 versus r for different depths (close to the depths of the measured currents plotted in Fig. S1) and latitudes (20°N, 30°N, 40°N). First, the currents at 30°N are much stronger than those at 20°N and 40°N, highlighting the significance of the resonance. Second, as expected, current speed decreases monotonically as a function of the friction coefficient, r, and this decrease is more pronounced for the deep currents. Third, the simulated currents during January 2009 are stronger than those of April 2009 for a small enough friction coefficient. The crossing point (indicated by the vertical dashed line in Fig. S2) between simulated January and April monthly mean current speed curves (green and blue curves in Fig. S2) is larger for deeper currents. This suggests a rather small upper bound for the friction coefficient, $r < 10^{-6}$ s^{-1}, obtained at a depth of 10 m (Fig. S2a), since in this range, the simulated January currents are larger than the simulated April currents, as in the observations (Fig. S1b). Alternatively, Fig. S2 may indicate that r is depth-dependent.

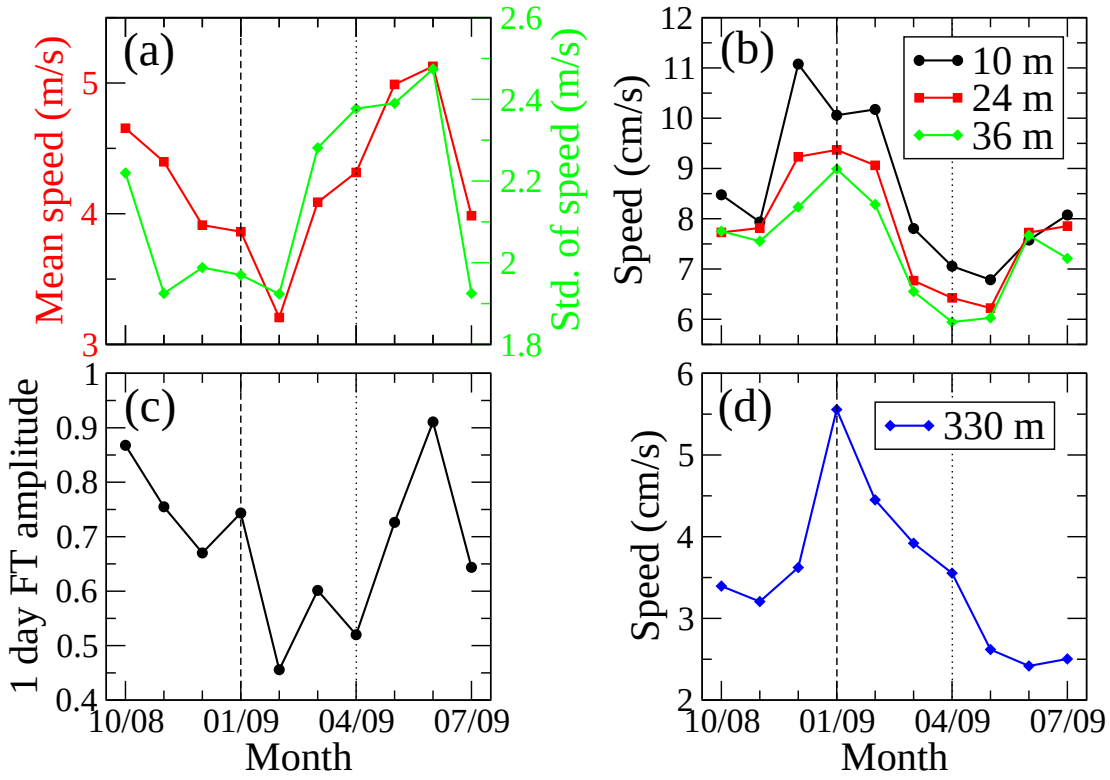

FIG. S1: (a) Monthly mean (red) and standard deviation of the wind speed (in m/s) from the Gulf of Elat (34.92°E, 29.5°N). (b) Monthly mean current speed (in cm/s) at different shallow depths. (c) FT amplitude of the wind speed at the diurnal frequency. (c) Monthly mean current speed (in cm/s) at a depth of 330 m. The vertical dashed line indicates January 2009 and the vertical dotted line indicates April 2009.

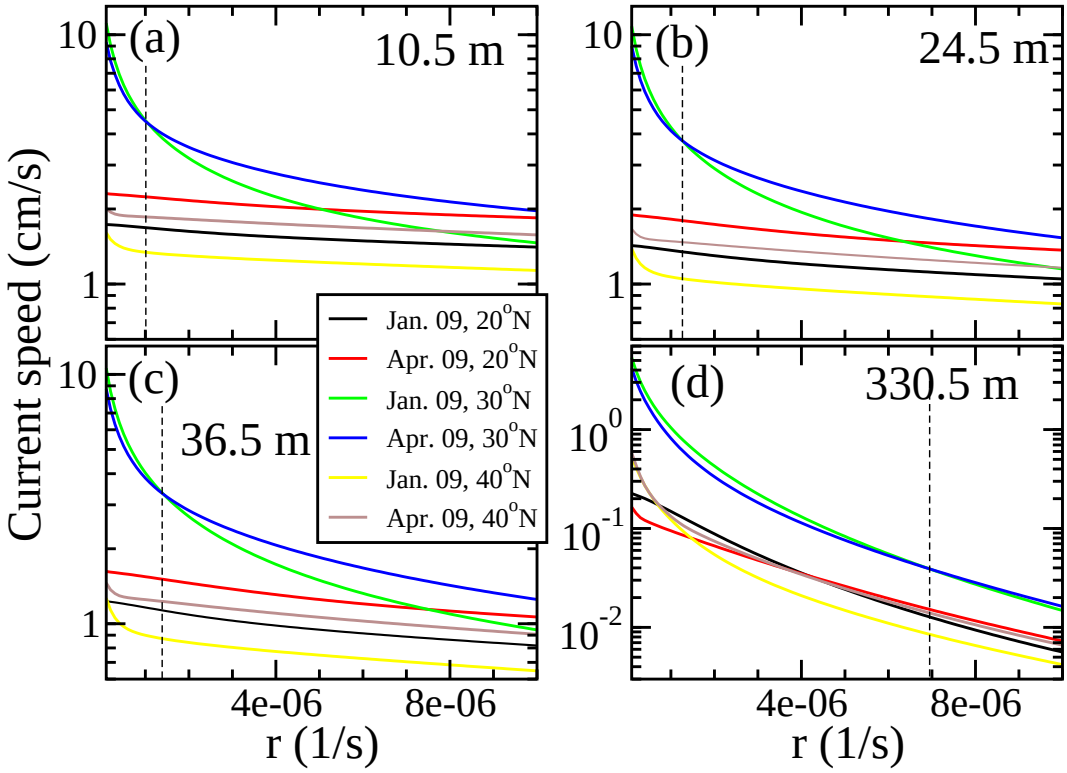

FIG. S2: Mean simulated current speed as a function of the friction coefficient, r, when forced by the observed winds of January and April 2009 from the Gulf of Elat, for different latitudes (20°N, 30°N, and 40°N) and depths: (a) 10.5 m, (b) 24.5 m, (c) 36.5, and (d) 330.5 m. The vertical dashed line indicates the transition point at which the mean current speed of January 2009 becomes smaller than that of April 2009.